

# Lattice dynamics of Ge and Si using the Born-von Karman model

A. D. Zdetsis\* and C. S. Wang

*Bartol Research Foundation of The Franklin Institute, University of Delaware, Newark, Delaware 19711*

(Received 31 May 1977; revised manuscript received 16 October 1978)

The Born-von Karman model of lattice dynamics of diamond structure has been extended to include up to 12th-neighbor interactions. Applications to Ge and Si using eighth-neighbor interactions have been carried out. We obtained very good fits to the experimental values of phonon dispersion curves and elastic constants. However, in agreement with the conclusions of Herman, a reasonable fit can only be obtained using at least up to fifth-neighbor interactions. The special significance of the fifth neighbor is attributed to its structure. With the fitted force constants, we have calculated the phonon density of states using the high-resolution Gilat-Raubenheimer method. The calculated Debye temperatures and specific heats compare well with the experimental values.

## I. INTRODUCTION

The theory of lattice dynamics can be traced back to 1907, when the theory of specific heats was published by Einstein.<sup>1</sup> The diamond structure was given great emphasis from the very beginning. Einstein originally applied his quantized oscillator model for specific heats to diamond. Diamond was one of the first crystal structures to be investigated by Born<sup>2</sup> using the celebrated theory of lattice dynamics developed by von Kármán and himself. Various extensions of their work appeared in later years,<sup>3-5</sup> and the model is known as the Born-von Karman model (BKM).

During the late 1950's the development of slow neutron scattering techniques pioneered by Brockhouse<sup>6</sup> made it feasible for the first time to obtain detailed information on the spectrum of lattice vibrations in a crystal. In addition to this, many optical measurements, such as infrared and first- and second-order Raman scattering, also give precise values of phonon frequencies at symmetry points of the Brillouin zone. Phonon frequencies at any point in the Brillouin zone can now be measured with an accuracy of better than 1% by many groups. Nilson and Nelin have obtained the most complete and accurate neutron scattering measurements for germanium.<sup>7,8</sup>

In this paper we would like to report a detailed study of the lattice dynamics of germanium and silicon using Born-von Karman model. Although many other models<sup>9-12</sup> have been proposed and the experimental data of Nilson and Nelin have been analyzed using some of these models,<sup>10-12</sup> to our knowledge no complete BKM study on their data has been reported.

In Sec. II we extend the formulation of the Born-von Karman model to include up to 12th-neighbor interactions. The complete dynamical matrix and equations for dispersion curves along major symmetry axes in the Brillouin zone are discussed in

this section. In Sec. III we describe the procedure for fitting the theoretical expressions to the measured phonon dispersion curves and elastic constants to obtain the force-constant parameters. Section IV uses the fitted force constants to calculate the phonon frequency distribution using the Gilat-Raubenheimer method. In Sec. V we use the phonon density of states to calculate the specific heat and Debye temperature to compare with experimental values. Finally, in Sec. VI, we discuss briefly the results and conclusions of the present study.

## II. DYNAMICAL MATRIX AND DISPERSION EQUATIONS

The Born-von Karman model (BKM) of the lattice dynamics of diamond lattices has been studied previously by many investigators. In particular, Smith<sup>4</sup> has the complete and detailed formulation for interactions up to second-neighbor atoms, and Herman<sup>5</sup> has extended this to sixth neighbors. Lax,<sup>13</sup> by proper choice of the origin of coordinates, has obtained much more simple forms of dynamical matrices up to fourth-neighbor interactions. He also obtained complete analytical expressions for the dispersion curves in the major symmetry directions.

There are only 12 independent matrix elements; among them only four elements are needed. All others can be obtained by cyclic permutation:

$$D_{11}^{kk'} \rightarrow D_{22}^{kk'} \rightarrow D_{33}^{kk'}; D_{12}^{kk'} \rightarrow D_{23}^{kk'} \rightarrow D_{31}^{kk'}. \quad (1)$$

The dispersion curves and phonon density of states can be obtained by solving the secular equation

$$|D(\vec{q}) - IM\omega^2| = 0, \quad (2)$$

where  $M$  is the atomic mass of Ge or Si and  $I$  is a  $6 \times 6$  unit matrix. Since the details of the dynamical matrix elements are available elsewhere,<sup>14</sup> we shall not repeat them here.

### III. FITTING TO THE MEASURED ELASTIC CONSTANTS AND DISPERSION CURVES

In order to determine the force-constant parameters, a nonlinear least-square fitting of the theoretical expressions to the measured elastic constants and dispersion curves must be used. We have adapted the nonlinear least-square fitting method of Marquardt<sup>15</sup> for this purpose. The Marquardt method, which combines analytical expansion method of linear least-square fitting and a gradient search method, has the advantage of achieving rapid convergence. The detailed description of the Marquardt method can be found in a book by Bevington.<sup>16</sup>

The experimental data used in the fitting process for Ge are those of Nilsson and Nelin.<sup>7</sup> We selected 70 evenly distributed points of the experimental dispersion curves along the  $\Lambda$ ,  $\Delta$ , and  $\Sigma$  directions, with five points from each branch. To these data the Raman frequency and the experimental values of the elastic constants<sup>17</sup> were added, raising the total number of fitted data to 74. For Si the experimental results were taken from the measurements of Nilsson and Nelin<sup>18</sup> and of Dolling and Dowley<sup>19</sup>; the former data are more accurate, whereas the latter are more complete. We used both sets of data in the fitting process. Wherever an overlap existed, we have chosen the more accurate data. For Si we fitted a total of 79 experimental data, including the Raman frequency and the elastic constants.<sup>17</sup> In Table I we list the best results of the fitting for Ge and Si. Since the experimental data for Ge are very accurate, with a sixth-neighbor fit we did not obtain a result which is within experimental uncer-

tainty; therefore, an eighth-neighbor fit was used. The variation of the fitting  $|\Delta\nu|_{\text{fit}}$  is reduced by a factor of 2 by using eighth-neighbor fit. For Si, the data are not as accurate; a sixth-neighbor fit is sufficient. In Table I we also list the average variations of the fitting and the corresponding experimental frequencies, and compare with the average experimental uncertainty  $|\Delta\nu|_{\text{exp}}$  and Raman frequencies  $\nu_R$ .

For both crystals, no satisfactory fit could be obtained using interactions out to fourth-order neighbors, which contain 12 force-constant (FC) parameters. It was found that the introduction of the third-neighbor interactions did not improve the quality of the second-neighbor fit substantially. Furthermore, fourth neighbors made only a marginal contribution. Nevertheless, as soon as the fifth-neighbor parameters were introduced, it became possible to obtain satisfactory fits. This is in accordance with the conclusions of Herman,<sup>5</sup> who, however, has used a considerably less accurate and incomplete set of data available at the time. The critical importance of the fifth neighbor can be traced to its special arrangement of atoms. The atoms in the second, third, and fourth neighbors are evenly distributed in all directions, while the fifth-neighbor atoms group behind the atoms in the first neighbor. Therefore, the fifth-neighbor atoms can supplement the deficiencies in the description of the interactions by only first-neighbor atoms, that cannot be corrected by the atoms in second through fourth neighbors. The special significance of the fifth-neighbor interactions in the BKM can also be seen in the table of FC parameters; the fifth-neighbor constant  $\lambda'''$  is

TABLE I. Best fitted force constants for Ge and Si ( $10^4$  dyne/cm).

		Ge	Si			Ge	Si
1°	$\alpha$	4.2197	4.5714	6°	$\mu''''$	0.0374	0.0147
	$\beta$	3.7528	4.2027		$\lambda''''$	-0.0243	-0.0237
	$\mu$	0.2349	0.3158		$\nu''''$	0.0288	0.0559
2°	$\lambda$	-0.5332	-0.6543		$\delta_+''''$	0.0242	-0.0055
	$\nu$	0.4166	0.5108		$\delta_-''''$	-0.0472	-0.0097
3°	$\delta$	0.1966	0.2658	7°	$\mu_7$	0.0013	...
	$\mu'$	0.0831	0.1241		$\lambda_7$	-0.0150	...
	$\lambda'$	-0.3371	-0.2620		$\nu_7$	-0.0138	...
	$\nu'$	-0.0481	-0.1797		$\delta_7$	-0.0382	...
	$\delta'$	-0.1677	-0.1563		$\mu_8$	-0.0525	...
4°	$\mu'''$	-0.1544	-0.0736	8°	$\lambda_8$	-0.0198	...
	$\lambda'''$	0.3798	0.1339		$\nu_8$	-0.0493	...
	$\mu''''$	0.1552	0.1512		$\delta_8$	0.0147	...
5°	$\lambda''''$	0.6007*	0.7455*			0.0362 THz	0.0580 THz
	$\nu''''$	0.0958	0.1057			0.0327 THz	0.0425 THz
	$\delta''''$	0.1760	0.2494			9.12 THz	15.00 THz

$$^a |\Delta\nu|_{\text{fit}} = \frac{1}{N} \sum_{i=1}^N |\nu(i)_{\text{fit}} - \nu(i)_{\text{exp}}|.$$

particularly large for Ge and Si.

In Fig. 1 we plotted the theoretical dispersion curves of germanium corresponding to the sets of force constants given in Table I. The experimental points are those of Ref. 7. The size of the experimental points are plotted according to the experimental errors quoted. We can see that, with the exception of  $\Sigma_3(0)$  branch, for which the calculated values are slightly higher than measured values, all other branches are fitted within the experimental accuracy. Our fitting to the experimental points using BKM is better than the fitting of other models reported.<sup>10-12</sup> However, the number of FC parameters involved in BKM is very large—29 for the eighth-neighbor fit (Ge) and 21 for the sixth-neighbor fit (Si).

#### IV. CALCULATION OF THE PHONON DENSITY OF STATES

There exist many different methods and interpolation formulas for calculating phonon density of state. These are described in considerably detail by Maradudin *et al.*<sup>20</sup> With large and fast computers available many of these methods can give sufficiently accurate calculations of the density states. However, among these methods the fastest and most accurate method is probably the analytical integration method of Gilat and Raubenheimer.<sup>21</sup> This method divides the irreducible sector of the Brillouin zone into many subzones and diagonalizes the dynamical matrix at the center

of each subzone. The frequencies near the subzone centers are then obtained by analytical interpolation. Thus it is equivalent to a much larger number of diagonalization. The detailed description of the method can be found in the original paper of Gilat and Raubenheimer.<sup>21</sup> One important feature that we have adopted in the program is a theorem concerning complex matrices.

Lax has shown that due to invariance under time reversal a complex matrix can be transformed to a real matrix by a unitary transformation.<sup>13</sup> Let

$$u = \frac{1}{\sqrt{2}} \begin{vmatrix} 1 & 1 \\ -i & i \end{vmatrix} \quad D = \begin{vmatrix} H & S \\ S^* & H^* \end{vmatrix};$$

then

$$D' = uDu^{-1} = \begin{vmatrix} \text{Re}(H+S) & \text{Im}(S-H) \\ \text{Im}(S+H) & \text{Re}(H-S) \end{vmatrix}$$

is a real matrix. Thus instead of diagonalization of a complex  $6 \times 6$  matrix, we need only diagonalize a  $6 \times 6$  real matrix. This reduces the computer time greatly. It takes less than 4 min of computer time on the IBM 370/168 to run a complete density of states calculation with a 3000 diagonalization of the dynamical matrix.

The results of our density of state calculation are shown in Figs. 2 and 3. The gross features of the density of state curves are similar to those of Tubino *et al.*<sup>10</sup> using valence force model and of Weber<sup>11</sup> using bound charge model, as well as to

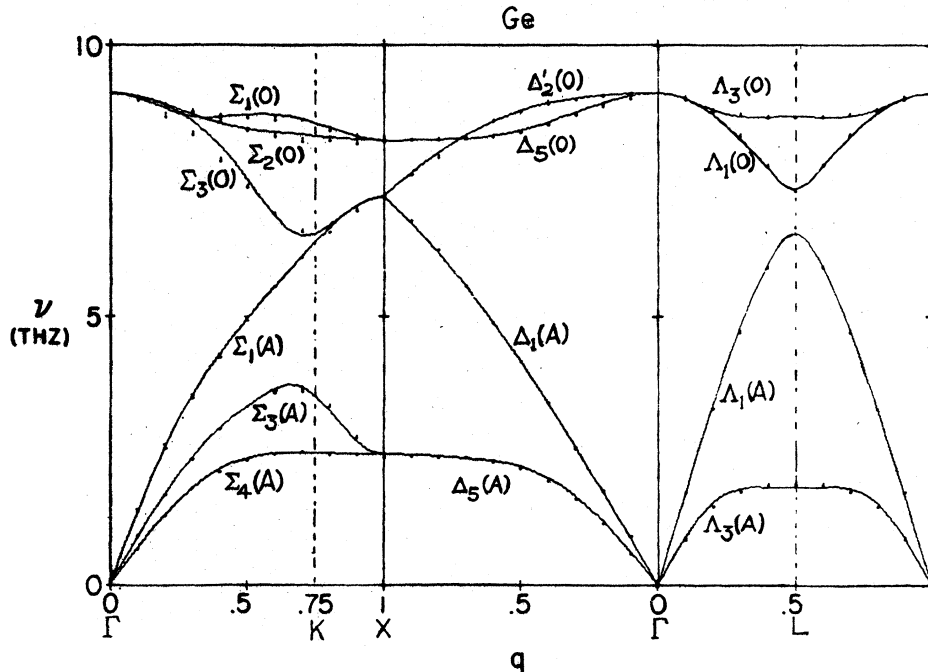


FIG. 1. Phonon dispersion curves of Ge (at 80 °K); the experimental points are from Nilsson and Nelin (Ref. 7). The solid curves are calculated from an eighth-neighbor fit (Table I) of Born-von Karman model to the experimental data.

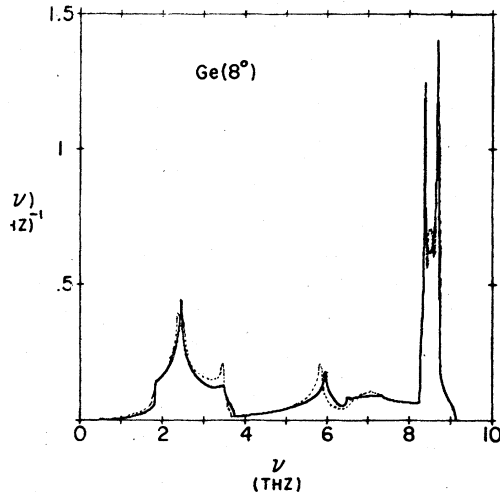


FIG. 2. Phonon density of states in Ge as a function of frequencies calculated with an eighth-neighbor Born-von Karman model (solid curve). The phonon density of state obtained by Nelin and Nilsson (Ref. 8) using extended sampling of neutron data is also included (broken curve).

those of Nelin and Nilsson<sup>8</sup> using extended sampling method of experimental data. However, our results represent considerable improvement in the numerical accuracy. Comparison with the shell model calculation<sup>19</sup> shows that there are discrepancies with the shell model result, especially in the acoustic part of the density of state curve. For the low-frequency portion of the density of state curve, the relative heights at various singular points agree with each other for the above-mentioned three calculations and with the second-order Raman spectrum,<sup>22-25</sup> while the shell model gives different relative peak heights.

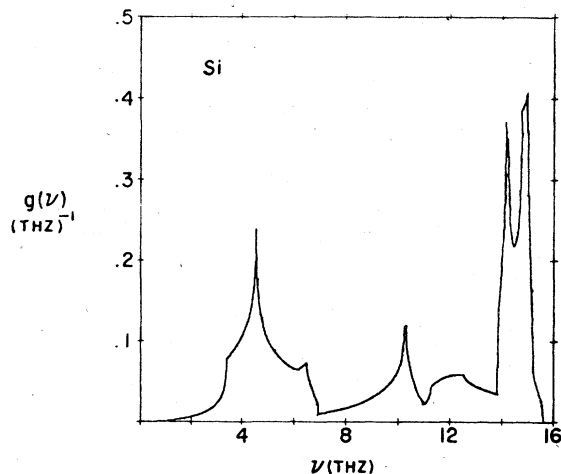


FIG. 3. Phonon density of states in Si as a function of frequencies calculated using a six-neighbor Born-von Karman model.

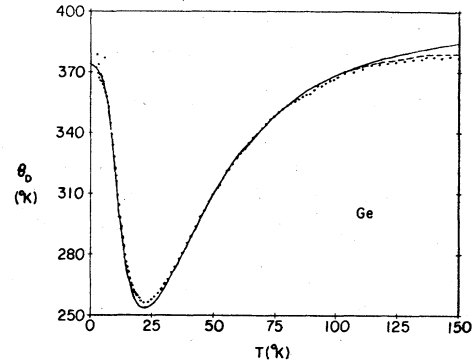


FIG. 4. Debye temperature of Ge as a function of absolute temperature. The solid curve is the result of BKM. The dotted curve is with anharmonic correction. Experimental points are those of Flubacher *et al.* (Ref. 26).

#### V. COMPARISON WITH THE MEASURED SPECIFIC HEAT DATA

The measurements of the specific heats of Ge and Si by Flubacher *et al.*<sup>26</sup> are also very accurate, which provides a stringent test for the phonon density of state calculations. In Figs. 4 and 5 we plotted the experimental values of Debye temperature as a function of temperature and compared them with the prediction of BKM using the density of state curve shown in Figs. 2 and 3. The calculated Debye temperature agrees with the experimental values to within 1% at all temperatures; at high temperature a systematic deviation from experimental values exists. This is expected, since BKM does not take into account the anharmonic effect.

The correction of the specific heat due to anharmonic effect can be evaluated if the temperature

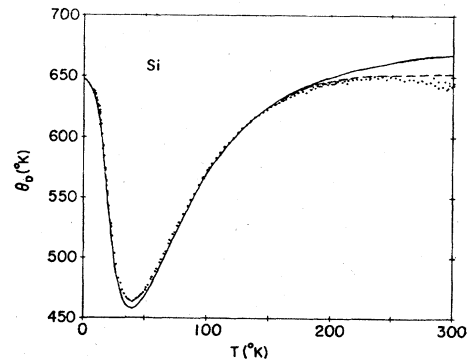


FIG. 5. Debye temperature of Si as a function of absolute temperature. The solid curve is the result of BKM. The dotted curve is in the anharmonic correction. Experimental points are those of Flubacher *et al.* (Ref. 26).

dependence of the phonon frequencies are known.<sup>27</sup> Since in BKM the phonon frequencies and the elastic constants are expressed in terms of the same set of force-constant parameters, the temperature dependence of phonon frequencies can be estimated from the temperature dependence of elastic constants. We have calculated the anharmonic correction to the specific heat using the temperature dependence of elastic constant measured by McSkimin.<sup>17</sup> The dotted curves in Fig. 4 and 5 show the Debye temperatures with anharmonic corrections.

## VI. DISCUSSIONS AND CONCLUSION

As shown in Sec. III, BKM is capable of obtaining very good fit to the accurately measured phonon dispersion curves as well as the elastic constants. Such a good fit is not achieved in previous attempts using different models.<sup>15-17</sup> For example, the valence force model<sup>15</sup> and bond charge model<sup>16</sup> have difficulties, that is, either elastic constants or a particular branch of phonon dispersion curve cannot be well fitted. There are a few parameters that are particularly important in obtaining a good fit in the BKM. For example, the second-neighbor parameter  $\lambda$  accounts for the large difference be-

tween longitudinal and transverse modes in the  $\Delta$  direction, while the fifth-neighbor parameter  $\lambda'''$  contribute strongly to the elastic constant  $C_{44}$ , and does not contribute significantly to other elastic constants or dispersion curves.

In conclusion, we have used Born-von Karman model to obtain very good fit to the measured phonon dispersion curves. The calculated Debye temperature agrees very well with the measured values. The agreement with other model calculations as well as with the second-order Raman spectrum are also very good. Since the errors introduced by the numerical analysis are negligible, our calculated phonon density of state presented in Figs. 2 and 3 should represent the true phonon density of states of Ge and Si to a very good accuracy.

## ACKNOWLEDGMENTS

We would like to thank Professor W. B. Daniels for stimulating discussions and Dr. M. Mostoller for communications with the Gilat and Raubenheimer method. We also thank the referee for suggesting many changes in the original manuscript, in particular, omission of the expressions for dynamical matrix elements and dispersion equations.

\*Present address: Nuclear Research Center Demokritos, Aghia Paraskevi Attikis, Athens, Greece.

<sup>1</sup>A. Einstein, *Ann Phys.* **22**, 186 (1907).

<sup>2</sup>M. Born, *Ann. Phys.* **44**, 605 (1914).

<sup>3</sup>G. H. Begbie and M. Born, *Proc. R. Soc. Lond. A* **188**, 179 (1947).

<sup>4</sup>H. M. J. Smith, *Philos. Trans. R. Soc. Lond. A* **241**, 105 (1948).

<sup>5</sup>F. Herman, *J. Phys. Chem. Solids* **8**, 405 (1959).

<sup>6</sup>B. N. Brockhouse and P. K. Iyengar, *Phys. Rev.* **111**, 747 (1958).

<sup>7</sup>G. Nilsson and G. Nelin, *Phys. Rev. B* **3**, 364 (1971).

<sup>8</sup>G. Nelin and G. Nilsson, *Phys. Rev. B* **5**, 3151 (1972).

<sup>9</sup>W. Cochran, *Phys. Rev. Lett.* **2**, 495 (1959).

<sup>10</sup>R. Tubino, L. Piseri, and G. Zerbi, *J. Chem. Phys.* **56**, 1022 (1972).

<sup>11</sup>W. Weber, *Phys. Rev. Lett.* **33**, 371 (1974); G. Nelin, *Phys. Rev. B* **10**, 4331 (1974); W. Weber, *Phys. Rev. B* **15**, 4789 (1977).

<sup>12</sup>G. Bose, B. B. Tripathi, and H. C. Gupta, *J. Phys. Chem. Solids* **34**, 1867 (1973); B. P. Pandey and B. Dayal, *Solid State Commun.* **11**, 775 (1972); *J. Phys. C* **6**, 2943 (1973).

<sup>13</sup>M. Lax, *Symmetry Principles in Solid State and Molecular Physics* (Wiley, New York, 1974).

<sup>14</sup>For interactions up to sixth neighbors see Refs. 5 and 13; for up to 12th neighbors see A. D. Zdetsis, thesis

(Thomas Jefferson University, 1976 (unpublished)).

<sup>15</sup>D. W. Marquardt, *J. Soc. Ind. Appl. Math.* **11**, 431 (1963).

<sup>16</sup>P. R. Bevington, *Data Reduction and Error Analysis for the Physical Sciences* (McGraw-Hill, New York, 1969).

<sup>17</sup>H. J. McSkimin, *J. Appl. Phys.* **24**, 988 (1953).

<sup>18</sup>G. Nilssen and G. Nelin, *Phys. Rev. B* **6**, 3772 (1972).

<sup>19</sup>G. Dolling and R. A. Cowley, *Proc. Phys. Soc. (Lond.)* **88**, 463 (1966).

<sup>20</sup>A. A. Maradudin, E. W. Montroll, G. H. Weiss, and I. P. Ipotova, *Theory of Lattice Dynamics in the Harmonic Approximation* (Academic, New York, 1971).

<sup>21</sup>G. Gilat and L. J. Raubenheimer, *Phys. Rev.* **144**, 390 (1966).

<sup>22</sup>P. A. Temple and C. E. Hathaway, *Phys. Rev. B* **7**, 3685 (1973).

<sup>23</sup>C. S. Wang, J. M. Chen, R. Becker, and A. Zdetsis, *Phys. Lett. A* **44**, 517 (1973).

<sup>24</sup>K. Uchinokura, T. Sekine, and E. Matsura, *J. Phys. Chem. Solids* **35**, 171 (1974).

<sup>25</sup>B. A. Weinstein and M. Cardona, *Phys. Rev. B* **7**, 2545 (1973).

<sup>26</sup>P. Flubacher, A. J. Leadbetter, and J. A. Morrison, *Philos. Mag.* **4**, 273 (1959).

<sup>27</sup>A. P. Müller and B. N. Brockhouse, *Can. J. Phys.* **49**, 704 (1971).